Sensors and Actuators A 241 (2016) 34–43

Contents lists available at ScienceDirect

Sensors and Actuators A: Physical

journal homepage: www.elsevier.com/locate/sna

Low frequency (LF) RFID sensors and selective transient feature extraction for corrosion characterisation

Ali Imam Sunny*, Gui Yun Tian*, Jun Zhang, Maninder Pal

School of Electrical and Electronic Engineering, Newcastle University, Newcastle upon Tyne, England NE1 7RU, United Kingdom

ARTICLE INFO

Article history:
Received 2 September 2015
Received in revised form 14 January 2016
Accepted 3 February 2016
Available online 12 February 2016

Keywords:
LF RFID
Feature extraction
Feature selection
Corrosion characterisation
Ferrite cores
Non-destructive testing and evaluation (NDT&E)

ABSTRACT

In this paper, Low Frequency (LF) RFID sensing system is used to characterise marine atmospheric corrosion on steel samples. Considering the conductivity and permeability variation in the corrosion layer, optimisation of sensing sensitivity and communication distance of commercial RFID tags placed on both coated and uncoated samples (exposure duration between 1 and 12 months) for impedance matching and appropriate operation frequencies are analysed. To balance the communication distance between RFID reader and tag and to match the impedance variation of RFID tags on metallic samples, a concept of wireless power transfer (WPT) through strongly coupled magnetic resonance (SCMR) method at RFID is applied. Static and transient features are extracted and selected to characterise corrosion. To enhance the sensing sensitivity to corrosion characterisation, further experimental studies have been carried out using ferrite sheets. The proposed LF RFID sensing system has been validated using commercial RFID tags with different feature extractions and selection of features for corrosion characterisation.

1. Introduction

Many industrial sectors including transportation, utilities, manufacturing, government and civil infrastructure have an urgent need for a method to detect corrosion before significant damage occurs. Corrosion is the destructive change of a metal and its properties by chemical or electrochemical reaction with its environment [1]. Deterioration of infrastructure due to corrosion is not just an economic issue, but can also jeopardise human safety [2]. The chemical process of corrosion leads to changes in properties such as electrical conductivity and magnetic permeability. Also coated steels may have surface roughness changes due to both corrosion and the delamination of the coating layer. All these various factors affect corrosion behaviour differently, hence, there is no such detection technique that can be applied in all cases but rather the detection capability and analysis can be enhanced [3]. As a result, corrosion testing and detection is an essential area in industry. Recent developments in metallic structures and materials have intensified the requirement for reliable corrosion detection and monitoring methods [4].

Numerous works have been done to study atmospheric corrosion and out of those maximum numbers of them are long term exposure concerned publications [5]. In order to determine corrosion rate and investigate protective properties of coating, electrochemical impedance spectroscopy (EIS) [6,7] can be used. Variation in atmospheric corrosion based on metal loss can be validated using lab based approaches which are time consuming and require a lot of preparation [8]. However, they are not a reliable solution for real-time measurement.

Recently, electromagnetic NDT&E methods have been used to investigate corrosion detection [9] and Structural Health Monitoring (SHM) [10]. Eddy current (EC) and pulsed eddy current (PEC), are the most commonly used techniques in the field of electromagnetic NDT&E. These techniques have a wide variety of applications including stress measurement [11], flaw detection [12], and corrosion characterisation [13,14]. Traditionally corrosion has been simulated artificially and modelled using a patch of pure metal loss which established a link between differential peak value feature and dimension of the metal loss [15–18]. Also, several features have been extracted from the transient response analysis in PEC in order to identify and classify the defects in both time-domain and frequency domain [19–21]. However, the sensitivity of EC and PEC techniques decreases with increasing lift-off distance between the probe and the sample surface. Also within corrosion layer or area, the conductivity and permeability are reduced compared with the metal surface [22]. Gotoh and Hirano have found that corro-

* Corresponding authors.
E-mail addresses: a.sunny@newcastle.ac.uk, ali_sn@hotmail.com (A.I. Sunny), g.y.tian@ncl.ac.uk (G.Y. Tian).

http://dx.doi.org/10.1016/j.sna.2016.02.010
0924-4247/

sion reduces the electrical conductivity and magnetic permeability in steel by the use of B-H curve [22]. The quantitative analysis is different from previous work where corrosion was considered as metal loss [16]. The majority of NDT techniques are limited when it comes to online in-situ monitoring under thick insulation layer. The passive RFID sensors demonstrate the potential of cheap, passive wireless sensing which can be permanently embedded into structures for long term monitoring. Previously passive LF commercial RFID tags have been used to see the monotonic behaviour with corrosion progression using the static response of the signal [23]. Using commercial RFID tags for sensing metallic material properties and defects, it is important to cope with the operational working ranges and quality factor variation caused by the metallic samples. In order to match the impedance, concept of wireless power transfer (WPT) through strongly coupled magnetic resonance (SCMR) method is applied at RFID. WPT can be mainly classified in three kinds, which include electromagnetic radiation mode, electric field coupling mode and magnetic field coupling mode. Based on the proposed RFID principle [23], magnetic field coupling is considered. Magnetic field coupling mode can be classified in two types, i.e. short-range electromagnetic induction and then mid-range SCMR. Though the efficiency and power transfer of SCMR are little lower, the transfer distance can achieve meter level. In 2007, MIT proposed SCMR that were able to transfer 60W wirelessly at a distance of 2 m with ~40% efficiency [24]. Other widely used SCMR applications include implantable medical sensors [25–27] and transportation applications for wireless charging [28,29].

This paper is an extension to previous work on LF RFID sensors system with consideration of impedance matching with signal transmission distance. It uses the static feature extraction of RFID response for corrosion detection [23] and feature extraction methods of PEC responses for corrosion classification and characterisation [30,31]. In this paper, conductivity and permeability changes of the corrosion region are considered using the LF RFID based sensing system and transient feature is extracted for robustness of the performance.

The rest of the paper is organised as follows. Firstly, integration of RFID principle with WPT methods is shown in Section 2. Next in Section 3, feature extraction methods and selection of features to determine conductivity and permeability changes are discussed. Section 4, shows the coated and uncoated sample design and the experimental setup. Features for coated and uncoated samples are extracted, compared and validated along with the sensitivity enhancement using ferrite sheet are discussed in Section 5. Finally conclusion and further work are outlined in Section 6.

2. Integration of RFID principle with WPT methods

2.1. RFID sensor principle

RFID system consists of a reader and a tag/transponder. The reader typically consists of a microcontroller alongside RF circuitry such as envelope detectors and filters which are required to transmit and receive RF energy. The reader transfer enough power to the tag to activate it and receive the data stored in the tags memory via response signal from the tag and then finally write data to tag's memory. Tags that have been used in this study are passive off-the shelf RFID tags. Passive tags get all their power from near field carrier signal generated by a reader via SCMR.

Eddy current sensor model in [32] can be applied for RFID sensors and LF RFID sensor in particular [23]. Commercial RFID tags are designed for non-metallic environments. For NDT&E applications e.g. corrosion characterisation on metallic samples, RFID tag's impedance needs be considered. Fig. 1 illustrates the model for RFID reader, tag and the detected sample. In Fig. 1(a) a capacitor is connected across the reader and the tag to form a resonant circuit and this thereby results in lower efficiency. The efficiency, sensitivity and separation distance between tag and reader coil are strongly dependent on resonant frequency and operational frequency.

The resonant frequency of tag coil is shifted when it comes in close proximity to metallic structures [33,34]. When an alternating current passes through the reader coil, primary magnetic field is produced. In metal proximity, eddy current is produced on the surface creating a secondary magnetic field opposite to that of the primary magnetic field. Thus causing an impedance mismatch [35] and eventually a change in mutual inductance M_{RT} which is shown as:

$$M_{RT} = \frac{\mu\pi N_1 N_2 (r_1 + r_2)^2}{2\sqrt{\left(r_1{}^2 + x_1{}^2\right)^3}} \quad (1)$$

where:

μ = permeability of free space

N_1 and N_2 = number of turns in the reader and tag coils respectively

r_1 *and* r_2 = radius of the reader and the tag coils respectively

x_1 = distance between the two coils

It can be seen that the reader and tag coils are represented by the inductors L_R and L_T which are coupled with mutual inductance M_{RT} and a coupling coefficient of K_{Reader} which is given by:

$$K_{Reader} = \frac{M_{RT}}{\sqrt{L_R . L_T}} \quad (2)$$

The quality factor without metallic structure can be approximately shown as:

$$Q = \frac{2\pi f_r L_T}{R_T} \quad (3)$$

where R_T and L_T are the resistance and self-inductance of the tag coil; R_M and L_M are the equivalent resistance and self-inductance of the metal shown in Fig. 1(a). R_M inversely depends on the eddy current path and conductivity of the metal, L_M depends on the eddy current path and permeability of the metal. Metal near the tag can be modelled as an additional parallel inductance L_M. Commercial RFID tags are designed to work in near resonant frequency. Due to the close proximity to the metallic sample, the eddy current produced will not only shift tag's resonant frequency but will also reduce reader coil's sensitivity. It can be seen from Fig. 2(a) that the resonant frequency on metal f_m will shift towards the free space resonance f_0 as corrosion develops. To reduce the effect of metal and eddy current influence which will ultimately reduce the quality factor of the tag, WPT concept is used in order to match the impedance and ferrite sheet is used to improve the quality factor of the RFID tag. Fig. 2(b) shows the experimental setup with the ferrite sheet (0.1 mm).

2.2. Wireless power transfer model for RFID

Strongly coupled systems can transfer energy efficiently. A standard SCMR system consists of four elements [24]. In SCMR system, the reader and the tag are inductively coupled to the resonator coils which results in high Q-factor resulting in high wireless power transfer efficiency. The reader is inductively coupled with a resonator coil. The resonator then exhibits a resonant frequency that coincides with the reader frequency and the Q-factor is maximum. Similarly, the second resonator coil exhibits a resonant frequency that coincides with the tag frequency. SCMR requires both the resonators to be resonant at the same frequency in order to achieve WPT efficiently. The resonant frequency f_r can be calculated by:

$$F_r = 1/(2\pi\sqrt{LC}) \quad (4)$$

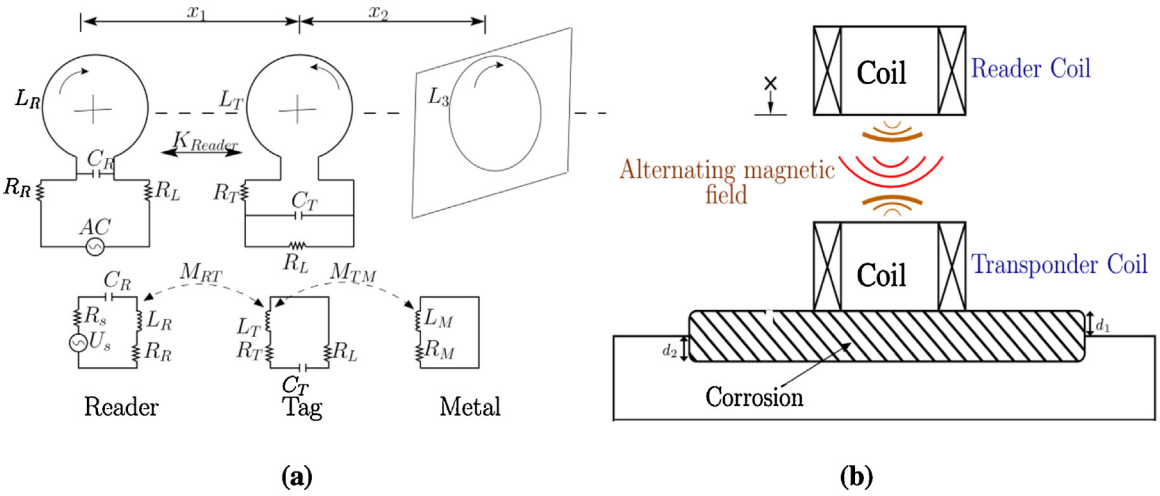

Fig. 1. (a) Inductive coupling principle between reader, tag and metal (b) schematic of RFID on corroded steel.

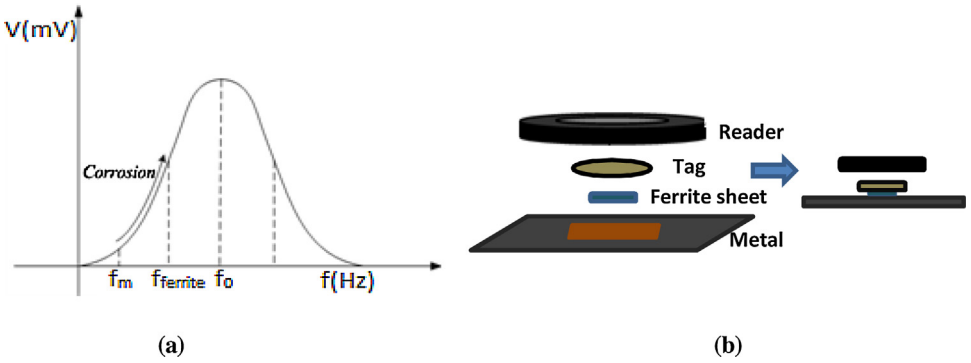

Fig. 2. (a) Operational frequency response curve and resonance frequency (b) setup using ferrite sheet.

Considering the resonators are identical coils, the efficiency of the SCMR system at its operational frequency can be shown as [36]:

$$\eta(f_r) = \frac{k^2_{(Tx-Rx)}(f_r)\,Q^2(f_r)}{1 + k^2_{(Tx-Rx)}(f_r)\,Q^2(f_r)} \tag{5}$$

where $k_{(Tx\text{-}Rx)}$ is the mutual coupling between the two resonator coils. In order to maximize the efficiency of a RFID system, the impedance needs to be matched for reader and the tag. In order to realize impedance matching, Fu et al. [37] proposed splitting frequency points in the odd or even mode which was only applicable for over coupled areas. Lee et al. [38] then proposed an anti-parallel resonant structure which can prevent coupling coefficient. This stabilizes the power transfer despite the change in distance. However this method discards, power transfer characteristics in close range. Chen et al. [39] and Duong et al. [40] proposed impedance matching method by adjusting the relative distance between adjacent coils. Based on this method, current experimental study on impedance matching carried out by adjusting the distance x_1 between the reader and the tag coils in order to attain proper working range as shown in Fig. 1(b). When there is a change in the distance x_1 between reader and the tag, there will be a corresponding change in impedance Z, inductance L and Q factor by mutual inductance M_{RT} according to:

$$\text{Z, L or} Q = f(x_1) \tag{6}$$

The theoretical analysis and experimental validation of the WPT concept for optimisation of signal 'communication' from tags to readers for metallic sample inspection will be discussed in another paper. The following section will concentrate on comparison of transient feature extraction and their sensitivity for corrosion characterisation from previous study [23].

3. Feature extraction and selection for corrosion characterisation

Many time domain features such as time to peak, amplitude of the peak, rising point and zero crossing, extracted from PEC responses have been used to classify and characterize defects on metallic objects [19,20,41]. In this section, two time domain features have been applied (i. e. transient and static response) from RFID response and analysed and are used to characterize the electrical conductivity and magnetic permeability of the corroded steel sample. Previous related studies on conductivity and permeability changes are shown in Refs. [11,12,41].

3.1. RFID response and feature extraction for corrosion characterisation

Pulse response of RFID is similar to that of PEC, a square wave, which contains rich frequency components. Different frequency components relate to different penetration depth information. The penetration depth in a conductive material is governed by the skin depth δ; this is shown in the equation (7)

$$\delta = 1/\sqrt{f\sigma\pi\mu} \tag{7}$$

where, f is the excitation frequency, σ is the electrical conductivity and μ is the magnetic permeability of the material. It can be seen

from the equation that as the frequency increases, the skin depth will decrease.

When testing with ferrous materials, the peak value of the measured magnetic field can vary significantly due to magnetisation effect. The feature characterizing the magnetic permeability variation is the maximum value of pulse *A,* which is the static value of the signal. In this paper, this characteristic is termed as *Max(A).* The transient response is the rising slope of the pulse which is shown as the first derivative of the signal i.e. $\delta A/\delta t$. Under such convention, a positive pulse of *A* due to the rising edge of excitation current means that the time constant T_c of corroded response decreases faster than that compared to non-corroded response, which corresponds to the decreasing electrical conductivity according to:

$$T_c = L/R \tag{8}$$

where L is the inductance and R is the resistance of the electrical circuit including the tag circuitry and the test sample.

As shown in Fig. 3, an increase in the positive pulse of *A* in Fig. 3(a) will result in the increase of *PVmax(δA/δt)* and decrease of *PVmin(δA/δt)* as shown in Fig. 3(b). This is attributed to the fact that as the corrosion progresses, the thickness of corrosion layer will increase [43] which subsequently reduce the electrical conductivity of the material [11,31,42]. Therefore, it can be inferred that *PVmax(δA/δt)* reflect the electrical conductivity change of the detected area of the material to be tested. Indication of reduced electrical conductivity caused by the difference of normalised signals from stress measurements in aluminium alloys have already been shown by previous researchers in [11,12].

In this section, two time domain features have been selected and are linked to the changes in electrical conductivity and magnetic permeability of the corroded region. In order to evaluate and compare the sensitivity of the features, other features have also been extracted and optimised in order to get a thorough comparison study. Amongst the seven features are, *Max(A)* which represents the maximum value of pulse A, *Adiff* which represents the difference between the maximum and minimum of the pulse and *Aedge* which represent the rising edge of the pulse and is defined by the upper and lower threshold of the rising edge denoted as M_2 and M_1, respectively. As for the differential measurements, the following were extracted, firstly the *PVmax(δA/δt)*, which represents the peak value of the $\delta A/\delta t$ and then the *PVmin(δA/δt)* which represents the minimum peak of $\delta A/\delta t$. Thirdly, the difference between the maximum peak and the minimum peak is found shown as *PVdiff(δA/δt)* and finally the pulse ratio which can be used to determine the quality factor of the signal is denoted as *Pratio(δA/δt)*which is defined as the reciprocal of the duty cycle. All these seven features (three from the pulse response and four from the differential of the pulse signal) are summarised, validated and compared to characterise corrosion (with and without ferrite sheet) in Section 5.

4. Sample design and experimental setup

Atmospheric corrosion of steel is a general term for an arrangement of iron oxides (hematite Fe_2O_3 and magnetite Fe_3O_4) and hydroxides (ferrous hydroxide Fe (OH) and ferric hydroxide Fe $(OH)_3$). Magnetite mostly in rust is developed in marine climates, which is a ferromagnetic mineral. Over time, only the proportions of the corrosion constituents have changes with little effect on the composition [43]. This is because density of pure steel is more than that of the iron oxides and hydroxides. During the early stage of the corrosion, the thickness of corrosion will increase but in the long-term corrosion it tends to decrease due to metal loss thereby changing the electrical conductivity and permeability. This work is focused on the characterization of early stage corrosion to determine the decrease in conductivity and permeability of corrosion region. Additionally, many steel companies apply coating on steel in order to prevent it from rusting; however, over time rust also develops under coating due to blistering or delamination. Based on these considerations, both uncoated and coated steel samples will be used and subsequently evaluated with RFID sensors using the proposed method. These have been provided by International Paint with atmospheric corrosion developed in marine atmosphere.

4.1. Corrosion progression samples

This set of samples consists of coated and uncoated mild steel plates (S275) which have different duration of atmospheric exposure (1, 3, 6, 10 and 12 months) to create different level of corrosion. The plates have dimensions of $300 \times 150 \times 3$ mm (length × width × thickness). A 30×30 mm rectangular patch at the centre of each plate was left exposed to allow rust to build up while the remainder of the plate was covered with plastic tape to keep the steel clean and dry. This then formed the uncoated samples. After that, half the plates were spray coated with epoxy phenolic based paint with a typical thickness of 100 μm. Images of coated and uncoated rust patches are shown in Fig. 4.

4.2. Experimental setup

A LF (125 kHz) RFID reader has been used to perform the experimental work. The tag used is ATA5577 from Atmel Corporation [44]. The tag is programmed with an ID consisting of '1's' at a data bit rate of 125 kHz/32 = 3.906 kHz with 50% duty cycles. Uniform stream of 1's have been chosen for easier processing as it allows averaging over many cycles. The position of the reader coil and the corrosion patch is maintained at a constant distance and aligned for each measurement while the tag is directly placed in the centre of the corrosion patch.

The signal from the reader coil is demodulated by the internal circuitry of the board in order to remove the 125 kHz carrier and noise. The circuit also includes an envelope detector which is then connected to an op-amp buffer. The output signal of the demodulation circuit is sampled using a 14-bit Adlink 2010 DAQ. The data acquisition is controlled in the PC using a LabVIEW program that allows the user to set the sample rate and number of samples to be acquired.

Experiments were carried out at different stand-off distances and 30 mm is found to be the optimum distance for the RFID tag to work best on the metallic samples This is because at a lower stand-off distance, the influence of the reader coil becomes higher than the tag whereas at a higher stand-off distance the tag coil cannot receive enough power from the reader coil thus reducing sensitivity to corrosion. The reader coil used is 90 mm in diameter with parameters of R = 10.45 Ω and L = 732 uH. Both the reader and the tag have resonant frequency of 125 kHz in free space. Due to the metal effect, the resonant frequency of the tag and reader becomes lower. However, the tag is influenced more than the reader since it is in direct contact with the metal surface. The output was sampled at 1 MHz for 0.01 s (10,000 data points). Fig. 5(a) shows the system setup along with the system diagram in Fig. 5(b).

5. Experimental results and validation

Based on the feature extraction and comparison study mentioned in section 3, it can be inferred that *Max(A)* feature can characterize permeability change and *PVmax(δA/δt)* can characterize conductivity variation and further features prove the robustness of the system and may be useful in future works for other applications. Measurements on uncoated and coated samples taken using the RFID system are shown in Sections 5.1 and 5.2 respectively. Section 5.3 shows the use of ferrite core to enhance sensitivity of the

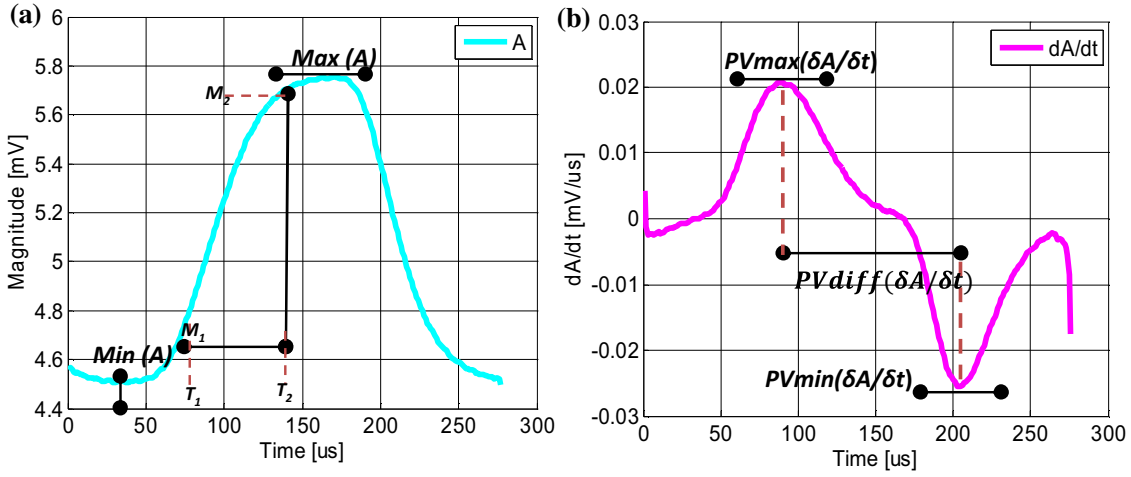

Fig 3. (a) RFID response of the proposed system on non-corroded metal, (b) differential response of Fig. 3 (a).

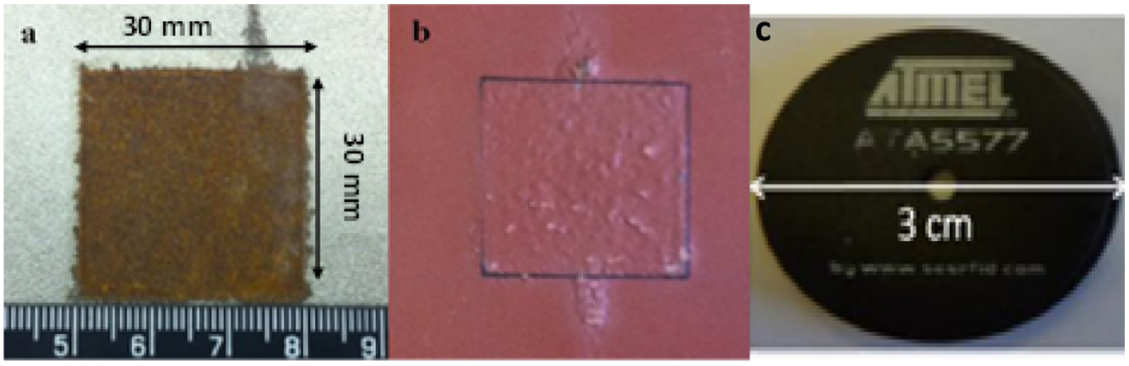

Fig. 4. Images of (a) 1 month uncoated, (b) 1 month coated rust patch (c) Commercial off-the-shelf tag.

response even further. The measurement was repeated 10 times for each sample and the average from those 10 measurements are then used as the measured value for further extraction.

To ease the feature selection, two equations are introduced and calculated i.e. the absolute variation Δ shown in Eq. (9), and the relative variation ε shown in Eq. (10). In tables, two specific samples i.e. 1 month and 6 months are represented as Sample 1 and Sample 6 respectively. These two samples are chosen for the comparison of absolute and relative variations because of their significant changes in exposure time. The absolute variation Δ between samples 6 and 1 is calculated by

$$\Delta = \text{max valve of sample 6} - \text{max value of sample 1} \quad (9)$$

Relative variation ε is calculated by

$$\varepsilon = (\Delta/\text{max value of sample})\,100 \quad (10)$$

5.1. Corrosion characterisation in uncoated samples

In Table 1, all the features have been described and extracted and a comparison between corrosion samples is shown. From the absolute and relative variation of peak values, it is found that transient response has shown 4 times higher sensitivity than that of the static response. The difference between the maximum and minimum values has shown twice as much better sensitivity for the transient response. This shows that transient features have better relative sensitivity than static features. Furthermore, transient features do not depend on the baseline which means that any uncertainty e.g. a change of mutual coupling of the two coils can be minimised increasing the stability when installed permanently for SHM. Fig. 6 shows the phenomenon of corrosion spreading into the surrounding metal as time increases. When corrosion expands, it creates a gap between the plastic tape and steel. The oxygen and water can therefore spread to the steel under the tape causing the rust to spread.

The two plots in Fig. 7 shows the changes in peak values (*Max(A)* and *PVmax(δA/δt)*) and the difference between the maximum and minimum (*Adiff* and *PVdiff(δA/δt)*) for both the static and transient responses respectively. The responses have been normalised for better comparison of static and transient features. A monotonic increase with exposure time can be seen from both the plots with very low error bars showing lower uncertainty of the data and an increased accuracy and robustness.

From Fig. 7(a) it can be seen that, both the static and the transient responses show a monotonic rise with the corrosion exposure time. Fig. 7(b) however shows a slight higher response with the transient response than the static response between 1 and 10 months. From both the figures above it can be noticed that, there is a drop in amplitude at 12 months for static response; whereas the transient response shows an enhanced sensitivity. This is because as the exposure time increases, the corrosion area also increases and when the latter happens, the rust layer loosen up and the flakes fall off as it expands. Thus subsequent corrosion spreads outward rather than increase in thickness.

5.2. Corrosion characterisation in coated samples

Coating and corrosion layer changes the dielectric properties of the material under test and as mentioned in Section 4, corrosion

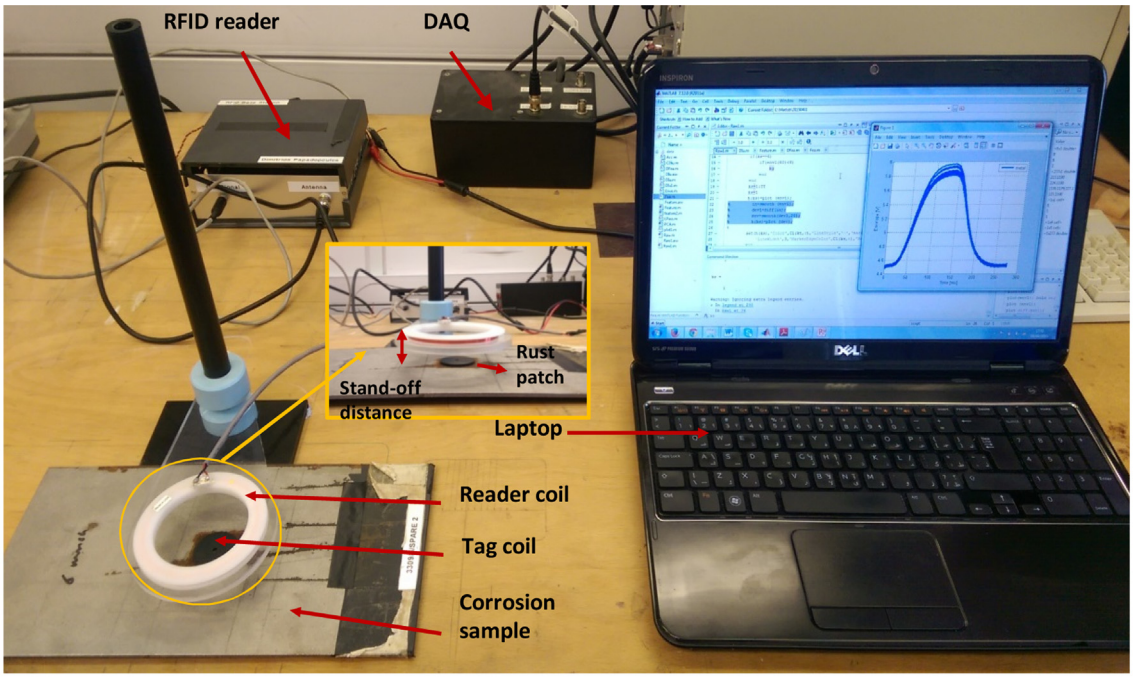

(a)

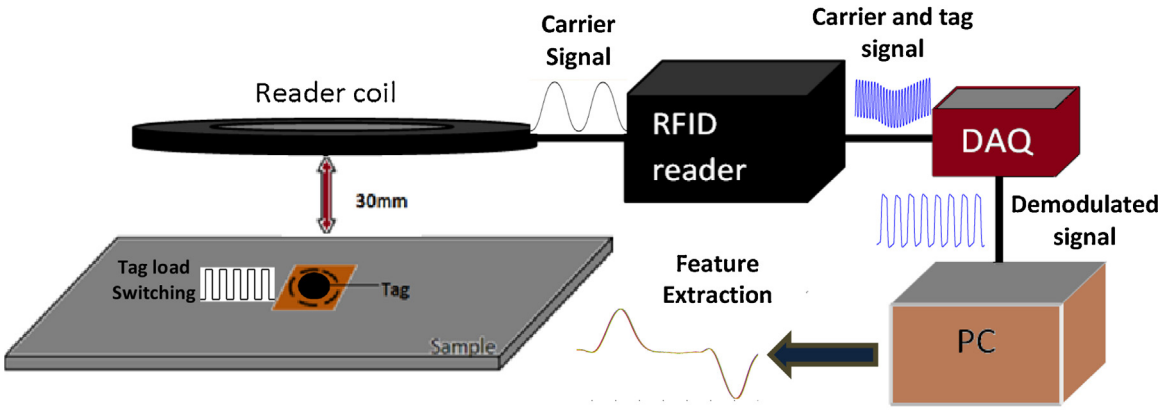

(b)

Fig. 5. (a) RFID system configuration for corrosion detection, (b) RFID system diagram.

Table 1
Features for corrosion on uncoated samples for 6 months and 1 month.

Features	Descriptions	Sample 6	Sample 1	Δ	ε (%)
Max(A)	Peak value of the pulse response	5.8678	5.8095	0.0583	0.99
Adiff	Difference between the maximum and minimum of the pulse slope	1.3463	1.3117	0.0346	2.57
Aedge	Rising edge of the pulse	0.0176	0.0166	0.0010	5.68
PVmax(δA/δt)	Maximum peak of the differential signal	0.0218	0.0209	0.0009	4.13
PVmin(δA/δt)	Minimum peak of the differential signal	−0.0253	−0.0240	−0.0013	5.14
PVdiff(δA/δt)	Difference between the maximum and minimum peak values of differential signal	0.0470	0.0445	0.0025	5.32
PVratio(δA/δt)	Difference between the maximum and minimum values of the differential signal over time to maximum and minimum values	−4.081e-04	−3.844e-04	−2.37e-05	5.81

also develops under coating, therefore in this section, coated samples are studied. Coating layer on the samples is approximately about 100 μm thick, hence the effect on RFID characterization is not very significant in comparison with the uncoated samples. This is because RFID system works on low operational frequency hence the dielectric property influence is small. This is also shown in the previous study using PEC carried out by He et al. in [31] where it was shown that there is a good agreement in the fitted lines of the measured values drawn between the coated and uncoated samples which are the same samples used in this study.

From Table 2, it can be seen that the relative variation between the two samples for the peak value is slightly higher than the

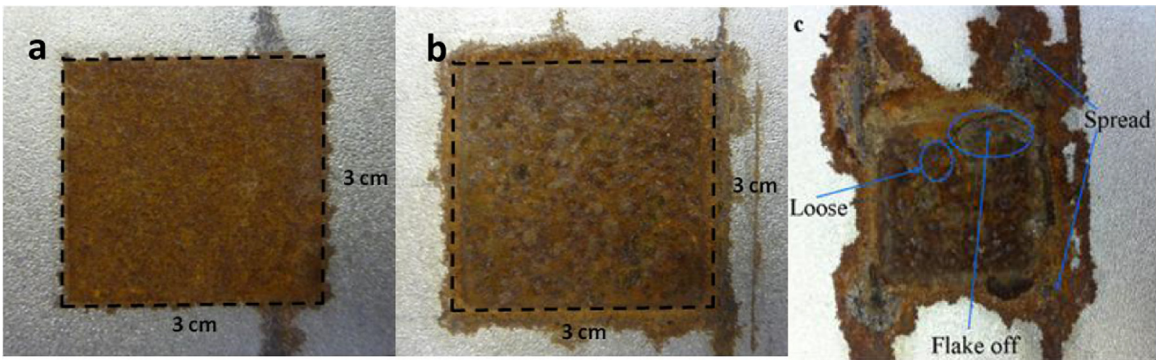

Fig. 6. Image of corrosion progression of (a) 1 month, (b) 6 months and (c) 10 months.

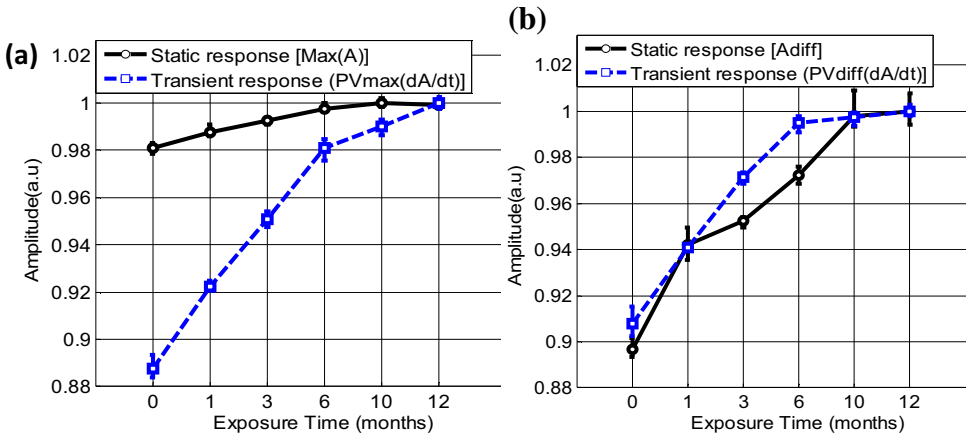

Fig. 7. Static and transient responses for uncoated samples showing (a) maximum value of responses (b) difference between the maximum and minimum of the pulse responses.

Table 2
Features for corrosion on coated samples for 6 months and 1 month.

Features	Sample 6	Sample 1	Δ	ε (%)
Max(A)	5.9426	5.8603	0.0823	1.38
Adiff	1.4536	1.3746	0.0790	5.43
Aedge	0.0185	0.0176	0.0009	4.86
PVmax(δA/δt)	0.0229	0.0219	0.0010	4.37
PVmin(δA/δt)	−0.0270	−0.0253	−0.0017	6.30
PVdiff(δA/δt)	0.0499	0.0471	0.0028	5.61
PVratio(δA/δt)	−4.304e-04	−4.068e-04	−2.36e-05	5.48

uncoated one. This is because the coating layer has prevented any flaking or metal loss and therefore the rust did not spread over the metal causing the thickness of the rust patch to be constant and hence the difference for the peak value between the two samples is higher. Also, the coating layer increases the lift-off between the transponder coil and the sample, thus reducing mutual coupling and therefore the shift in the resonant frequency is smaller.

Both Fig. 8(a) and (b) shows a similar pattern with the static and transient responses over the exposure time. A slight drop in amplitude can be noticed in the 3rd month for both the figures which is thought to be due to the uncertainty of the static response which is however enhanced using the transient response as it shows higher sensitivity. A monotonic trend with exposure time remains. However due to the 10th month's sample deformation as the sample has been receded from its original state, the sensitivity measurement value has dropped slightly for both features.

As illustrated in Fig. 7 and Fig. 8, the measured values for uncoated and coated samples are relative. Over time, an increase in the corrosion thickness means an increase in the corrosion contribution to the RFID responses; this lead to a reduction of the electrical conductivity and permeability of the corroded region.

5.3. Sensitivity and robustness enhancement using ferrite substrate

As shown in Fig. 2, that using a ferrite core will shift the tag's resonant frequency $f_{ferrite}$ towards the free space resonance f_0 which is the most sensitive working range. In this section further experimental study is carried out to enhance the performance of the RFID response using a ferrite core for further corrosion characterisation as shown in Fig. 9. From Sections 5.1 and 5.2, it can be seen that the relative sensitivity is improved by transient feature selection. Using the rising edge of the transient response (*PVmax(δA/δt)*), the sensitivity can be increased by about 3–4 times compared to the static response (*Max(A)*) for both coated and uncoated samples respectively. Previous work on both LF and UHF RFID has proved the enhancement of near field coupling using ferrite substrates for RFID applications [45,46].

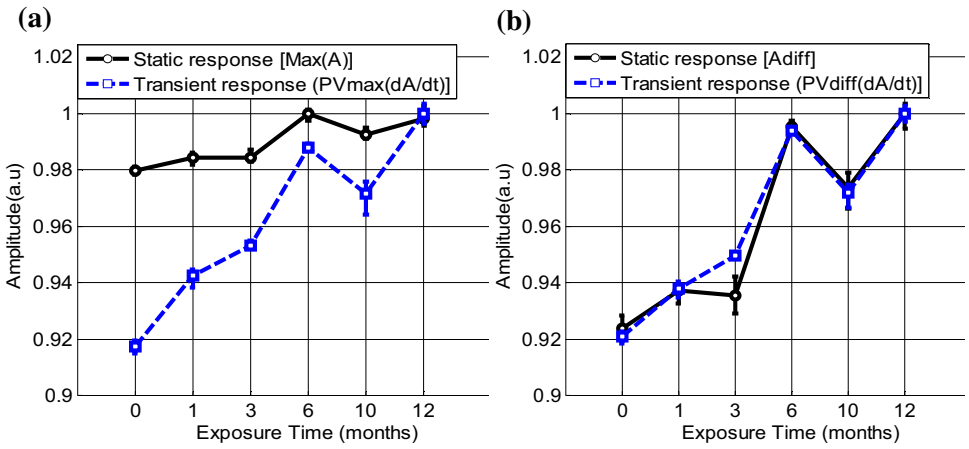

Fig. 8. Static and transient responses for coated samples showing (a) maximum value of the responses (b) difference between the maximum and minimum of the pulse responses.

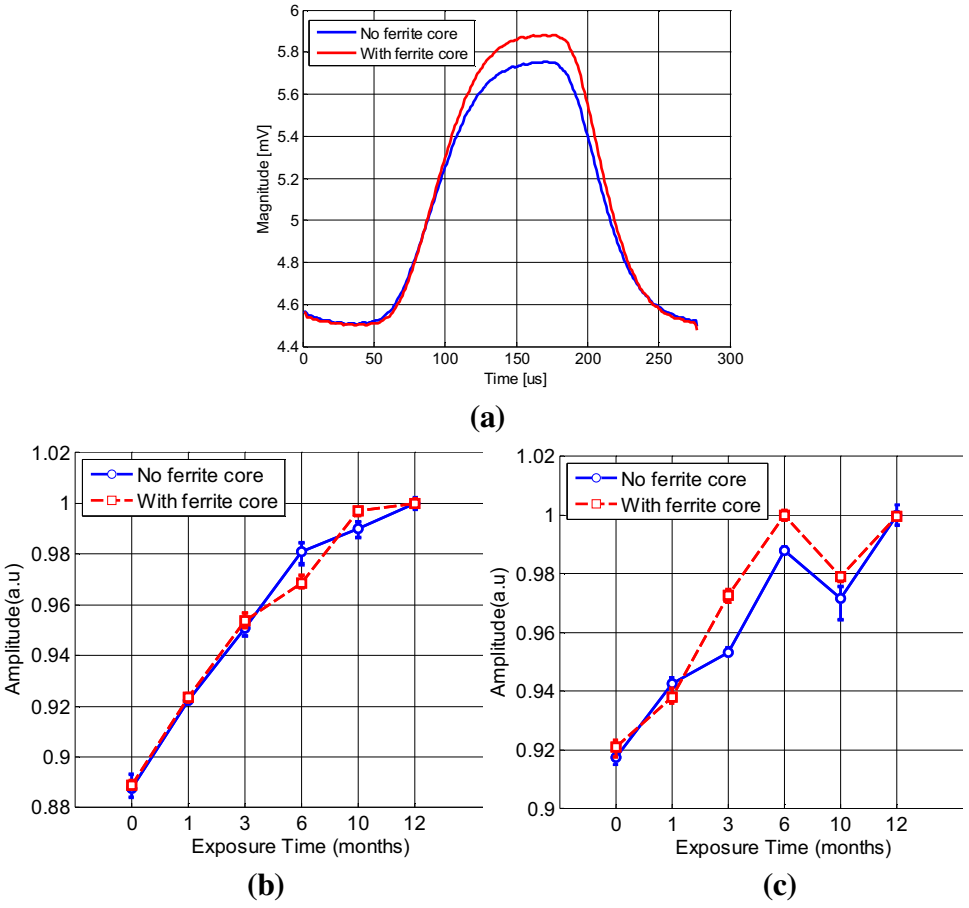

Fig. 9. (a) Pulse response on non-corroded metal (b) transient response for both with and without ferrite core on uncoated sample (c) transient response for both with and without ferrite core on coated sample.

Table 3
Comparison of uncoated and coated samples with and without ferrite core.

	Sample type	Features	Sample 6	Sample 1	Δ	ε (%)
No ferrite core	Uncoated	*Max(A)*	5.8678	5.8095	0.0583	0.99
		PVmax(δA/δt)	0.0218	0.0209	0.0009	4.13
	Coated	*Max(A)*	5.9426	5.8603	0.0823	1.38
		PVmax(δA/δt)	0.0229	0.0219	0.0010	4.37
With ferrite core	Uncoated	*Max(A)*	5.9916	5.9124	0.0792	1.32
		PVmax(δA/δt)	0.0242	0.0231	0.0011	4.55
	Coated	*Max(A)*	5.9866	5.8770	0.1096	1.83
		PVmax(δA/δt)	0.0256	0.0240	0.0016	6.25

Measurements in Table 3 shows that using ferrite cores, sensitivity is further improved even when compared to transient responses. However it needs to be kept in mind that the changes in absolute variation are small since the tag is commercial therefore the amplitude variation between samples are also small. Even with commercial tags, an increase of ~10–45% for both uncoated and coated specific samples respectively have been achieved. Further work will be carried out on tag fabrication for LF RFID with ferrite core or rod. It is expected that sensitivity and detection distance can be further improved by taking into consideration of the shift in resonant frequencies caused by metallic samples, lift-off distances and coupling factors of tag and readers.

6. Conclusion and future work

In this paper, both coated and uncoated mild steel samples with corrosion exposure between 1 to 12 months have been measured using proposed LF RFID system. The concept of WPT is applied in order to attain the working range for RFID sensing system. Also the distance between the reader and the tag is adjusted to match the impedance variation of commercial RFID tag on metallic sample. Several features are extracted and compared. Two features have been selected, namely static (*Max (A)*) and transient (*PVmax(δA/δt)*) response to determine permeability and conductivity changes respectively with corrosion exposure. From selected features, transient responses have proven to be significantly more sensitive and robust with corrosion progression compared to conventional static features.

Further prediction in terms of increasing sensitivity of the tag has been shown using ferrite cores with an enhanced pulse response from which more useful features related to corrosion characterisation can be extracted. An additional about 10–45% increase in sensitivity has been estimated using ferrite core without changing the distance between the RFID reader and the tag. Further sensitivity enhancement can be expected using WPT concept by optimally adjusting the distance between the reader and the tag.

Future work will include, designing of miniaturized transponder coils with enhanced sensitivity using proposed approach of ferrite cores as well as enhancing the communication distance with WPT and impedance matching and calibration for industrial applications.

Acknowledgements

The author would like to thank the International Paint Ltd, Gateshead, Newcastle, U.K for providing the experimental samples and EPSRC to fund the study. The author would also like to thank Dr Lok Woo, Dr Ahmed Sabaawi and research colleagues for useful discussion.

References

[1] P. Kritzer, Corrosion in high-temperature and supercritical water and aqueous solutions: a review, J. Supercrit. Fluids 29 (2004) 1–29.
[2] B. Goldie, K. Kapsams, Corrosion under insulation: basics and resources for understanding, JPCL (2009) 34–37.
[3] G.S. Frankel, N. Sridhar, Understanding localized corrosion, Mater. Today 11 (2008) 1138–1144.
[4] P.A. Schweitzer, Metallic Materials: Physical, Mechanical, and Corrosion Properties, Marcel Dekker, New York, 2003.
[5] P. Johnson, M.A. Winterbottom, G.C. Wood, Short term atmospheric corrosion of mild steel at two weather and pollution monitored sites, Corros. Sci. 17 (8) (1977) 691–700.
[6] M. Hattori, A. Nishikata, T. Tsuru, EIS study on degradation of polymer-coated steel under ultraviolet radiation, Corros. Sci. 52 (6) (2010) 2080–2087.
[7] V.F. Lvovich, Impedance Spectroscopy: Applications to Electrochemical and Dielectric Phenomena, (2012).
[8] G. Malumbela, M. Alexander, P. Moyo, Steel corrosion on RC structures under sustained service loads a critical review, Eng. Struct. 31 (11) (2009) 2518–2525.
[9] M.E. Davoust, L. Le Brusquet, G. Fleury, Robust estimation of hidden corrosion parameters using an eddy current technique, J. Nondestruct. Eval. 29 (3) (2010) 155–167.
[10] H.A. Sodano, Development of an automated eddy current structural health monitoring technique with an extended sensing region for corrosion detection, Struct. Health Monit. 6 (2) (2007) 111–119.
[11] M. Morozov, G.Y. Tian, P.J. Withers, Noncontact evaluation of the dependency of electrical conductivity on stress for various Al alloys as a function of plastic deformation and annealing, J. Appl. Phys. 108 (2) (2010) 024909-1–024909-9.
[12] G.Y. Tian, A. Sophian, D. Taylor, J. Rudlin, Multiple sensors on pulsed eddy-current detection for 3-D subsurface crack assessment, IEEE Sens. J. 5 (1) (2005) 90–96.
[13] T.W. Krause, D. Harlley, V.K. Babbar, K. Wannamaker, Pulsed eddy current thickness measurement of selective phase corrosion on nickel aluminium bronze valves, AIP Conference Proceedings (2010) 401–408.
[14] Y.A. Plotnikov, W.J. Bantz, J.P. Hansen, Enhanced corrosion detection in airframe structures using pulsed eddy current and advanced processin, Mater. Eval. 65 (65) (2007) 403–410.
[15] S.X. Liu, W. Xin, K.Q. Ding, Simulation of corrosion on detection for pulsed eddy current, Proc. 7th International Conference. Fuzzy System Knowledge Discovery (2010) 1839–1842.
[16] R.A. Smith, G.R. Hugo, Transient eddy current NDE for ageing aircraft capabilities and limitations, Insight-Non-Destr. Test. Cond. Monit. 43 (January (1)) (2001) 14–25.
[17] Y. He, F. Luo, M. Pan, Defect characterisation based on pulsed eddy current imaging technique, Sens. Actuators. A: Phys. Sep. 164 (2010) 1–7.
[18] R.A. Smith, D. Edgar, J. Skramstad, J. Buckley, Enhanced transient eddy current detection of deep corrosion, Insight-Non-Destr. Test. Cond.Monit. 46 (2) (2004) 88–91.
[19] Y. He, F. Luo, M. Pan, X. Hu, J. Gao, B. Liu, Defect classification based on rectangular pulsed eddy current sensor in different directions, Sens. Actuators. A: Phys 157 (1) (2010) 26–31.
[20] G.Y. Tian, A. Sophian, Defect classification using a new feature for pulsed eddy current sensors, NDT E Int. 38 (1) (2005) 77–82.
[21] Y. He, M. Pan, F. Luo, Reduction of lift-off effects in pulsed eddy current for defect classification, IEEE Magn. Trans. 47 (December (12)) (2011) 4753–4760.
[22] Y. Gotoh, H. Hirano, M. Nakano, K. Fujiwara, N. Takahashi, Electromagnetic nondestructive testing of rust region in steel, IEEE Trans. Magn. 41 (October (10)) (2005) 3616–3618.
[23] M. Alamin, G.Y. Tian, A. Andrews, P. Jackson, Corrosion detection using low-frequency RFID technology, Insight-Non-Destr. Test. Cond. Monit. 54 (2) (2012) 72–75.
[24] A. Kurs, A. Karalis, R. Moffatt, J.D. Joannopoulos, P. Fisher, M. Soljacic, Wireless power transfer via strong coupled magnetic resonances, Science 317 (5834) (2007) 83–86.
[25] X.H. Li, H.R. Zhang, F. Peng, Y. Li, T.Y. Yang, B. Wang, D.M. Fang, A wireless magnetic resonance energy transfer system for micro implantable medical sensors, Sensors 12 (2012) 10292–10308.
[26] C.-W. Chang, K.-C. Hou, L.-J. Shieh, S.-H. Hung, J.-C. Chiou, Wireless powering electronics and spiral coils for implant microsystem toward nanomedicine diagnosis and therapy in free-behavior animal, Solid-State Electron. 77 (2012) 93–100.
[27] Q. Xu, H. Wang, Z. Gao, Z.-H. Mao, J. He, M. Sun, A novel mat-based system for position-varying wireless power transfer to biomedical implants, IEEE Trans. Magn. 49 (2013) 4774–4779.
[28] J. Sallan, J.L. Villa, A. Llombart, J.F. Sanz, Optimal design of ICPT systems applied to electric vehicle battery charge, IEEE Trans. Ind. Electron. 56 (2009) 2140–2149.
[29] J.L. Villa, J. Sallán, A. Llombart, J.F. Sanz, Design of a high frequency inductively coupled power transfer system for electric vehicle battery charge, Appl. Energy 86 (2009) 355–363.
[30] T. Chen, G.Y. Tian, A. Sophian, P.W. Que, Que Feature extraction and selection for defect classification of pulsed eddy current NDT, NDT E Int. 41 (6) (2008) 467–476.
[31] Y. He, G.Y. Tian, H. Zhang, M. Alamin, A. Simm, P. Jackson, Steel corrosion characterisation using pulsed eddy current systems, IEEE Sens. J. 12 (6) (2012) 2113–2120.
[32] G.Y. Tian, Z.X. Zhao, R.W. Baines, The research of inhomogeneity in eddy current sensors, Sens. Actuators A: Phys. 69 (1998) 148–151.
[33] J. Kim, H.C. Son, K. Kim, Y. Park, Efficiency analysis of magnetic resonance wireless power transfer with intermediate resonant coil. antennas and wireless propagation letters, IEEE 10 (1) (2011) 389–392.
[34] K. Sasaki, S. Sugiura, H. Iizuka, Distance adaptation method for magnetic resonance coupling between variable capacitor-Loaded parallel-Wire coils. microwave theory and techniques, IEEE Trans. 62 (4) (2014) 892–900.
[35] D. Ciudad, P.C. Arribas, P. Sanchez, C. Aroca, RFID in metal environments: an overview on low (LF) and ultra-Low (ULF) frequency systems, in: Radio Frequency Identification Fundamentals and Applications Design Methods and Solutions, InTech, 2010.
[36] A.K. RamRakhyani, S. Mirabbasi, Chiao Mu, Design and optimization of resonance-Based efficient wireless power delivery systems for biomedical implants, IEEE Trans. Biomed. Circuits Syst. 5 (1) (2011) 48–63.

[37] W. Fu, B. Zhang, D. Qiu, Study on frequency-tracking wireless power transfer system by resonant coupling, in: Proceedings of the Power Electronics and Motion Control Conference (IPEMC '09), Wuhan, China, 2009, pp. 2658–2663.
[38] W.-S. Lee, W.-I. Son, K.-S. Oh, J.-W. Yu, Contactless energy transfer systems using antiparallel resonant loops, IEEE Trans. Ind. Electron. 60 (2013) 350–359.
[39] C.-J. Chen, Tah-H. Chu, C.-L. Lin, Z.-C. Jou, A study of loosely coupled coils for wireless power transfer, IEEE Trans. Circuits Syst. II: Express Briefs 57 (2010) 536–540.
[40] T.P. Duong, J.-W. Lee, Experimental results of high-efficiency resonant coupling wireless power transfer using a variable coupling method, IEEE Microw. Wirel. Compon. Lett. 21 (2011) 442–444.
[41] D. Zhou, G.Y. Tian, B. Zhang, M. Morozov, H. Wang, Optimal features combination for pulsed eddy current NDT, NDT. Eval. 25 (2) (2010) 133–143.
[42] M. Morozov, G.Y. Tian, P.J. Withers, The pulsed eddy current response to applied loading of various aluminium alloys, NDT E Int. 43 (6) (2010) 493–500.
[43] D. Fuente, I. Diaz, J. Simancas, B. Chico, M. Morcillo, Long-term atmospheric corrosion of mild steel, Corros. Sci. 53 (2) (2011) 604–617.
[44] Atmel ATA5577 Data sheet, (Online) Available: <www.atmel.com> (accessed June 2015).
[45] A. Tran, M. Bolic, M.C.E. Yagoub, Magnetic-field coupling characteristics of ferrite-coil antennas for low-frequency RFID applications, Int. J. Comput. Sci. 4 (1) (2010) 7–11.
[46] C. Stergiou, E. Eleftheriou, V. Zaspalis, Enhancement of the Near-field UHF RFID with ferrite substrates, IEEE Trans. Magn. 48 (4) (2012) 1497–1500.

Biographies

Ali Imam Sunny received his B.Sc. in Electrical and Electronic Engineering from Northumbria University (UK) in 2013. Currently he is pursuing his Ph.D. degree in ComS^{2}IP group at School of Electrical and Electronic Engineering, Newcastle University, United Kingdom. His research interests are focused on, RFID technology & applications, NDT&E and digital signal processing.

Gui Yun Tian received his B.Sc. degree and M.Sc. degree from University of Sichuan, Chengdu, China in 1985 and 1988, respectively, and Ph.D. from University of Derby, Derby, UK, in 1998. He is currently the Professor of Sensor Technologies at School of Electrical and Electronic Engineering, Newcastle University, United Kingdom. His main interests include Electromagnetic sensors, sensor array and sensor network, Electromagnetic Non-destructive Evaluation, Advanced signal processing and Integrative systems and applications. He has coordinated several research projects from the Engineering and Physical Sciences research Council (EPSRC), Royal Academy of Engineering and FP7. Also he has good collaboration with leading industrial companies such as Airbus, Rolls Royce, BP, nPower, Network Rail and TWI among others.

Jun Zhang (M'15) received the B.Sc. degree in information engineering from the South China University of Technology (SCUT), Guangzhou, in 2008, and the Ph.D. degree in radio physics from Sun Yat-sen University (SYSU), Guangzhou, in 2013. He is currently a research associate in the ComS^{2}IP group, Newcastle University. His research interests include antenna theory and design, RFID technology & applications, and NDT&E.

Maninder Pal obtained his B.Tech in Electronics & Communication Engineering from NIT, Kurukshetra, India in 2000 and MSc in Digital Communication from Loughborough University in 2004. He carried out his research work in the area of signal processing and was awarded Ph.D. in 2008 by Loughborough University. He worked for several years on various international organisations in the domain of acoustics and signal processing. Presently, he is working as Research Associate in the School of Electrical and Electronics Engineering of Newcastle University, United Kingdom